

Brain Extraction comparing Segment Anything Model (SAM) and FSL Brain Extraction Tool

Sovesh Mohapatra^{1,2}, Advait Gosai², Gottfried Schlaug^{1,3,4*}

¹Institute of Applied Life Sciences, University of Massachusetts, Amherst, 01003, MA.

²Manning College of Information and Computer Sciences, University of Massachusetts, Amherst, 01003, MA.

³Department of Biomedical Engineering, University of Massachusetts, Amherst, 01003, MA.

⁴Department of Neurology, Baystate Medical Center, and UMass Chan Medical School - Baystate Campus, Springfield, 01107, MA.

*Corresponding author(s). E-mail(s): gschlaug@gmail.com;

Abstract

Brain extraction is a critical preprocessing step in almost every neuroimaging study, enabling accurate segmentation and analysis of Magnetic Resonance Imaging (MRI) data. FSL's Brain Extraction Tool (BET), although considered the current gold standard, presents limitations such as over-extraction, which can be particularly problematic in brains with lesions affecting the outer regions, inaccurate differentiation between brain tissue and surrounding meninges, and susceptibility to image quality issues. Recent advances in computer vision research have led to the development of the Segment Anything Model (SAM) by Meta AI, which has demonstrated remarkable potential across a wide range of applications. In this paper, we present a comparative analysis of brain extraction techniques using BET and SAM on a variety of brain scans with varying image qualities, MRI sequences, and brain lesions affecting different brain regions. We find that SAM outperforms BET based on several metrics, particularly in cases where image quality is compromised by signal inhomogeneities, non-isotropic voxel resolutions, or the presence of brain lesions that are located near or involve the outer regions of the brain and the meninges. These results suggest that SAM has the potential to emerge as a more accurate and precise tool for a broad range of brain extraction applications.

Keywords: Brain Extraction, FMRIB Software Library, Segment Anything Model, Deep Learning

1 Introduction

Brain extraction from Magnetic Resonance Imaging (MRI) or other imaging techniques is an important preprocessing step to advance various other image segmentation tasks [1]. This process involves isolating brain tissue from non-brain tissues, such as the skull, scalp, and meninges, while preserving brain tissue that might have been altered due to various types of lesions or injuries, enabling accurate and effective subsequent processing [2–4]. Automatic and user independent brain extraction is challenged when brain tissue or non-brain tissue have similar or inhomogeneous signal intensity, leading to confusion of what constitutes brain tissue. The accurate removal of non-brain tissue enables automatic brain segmentation models to achieve significantly higher accuracy, and the reduction in information being processed enhances computational efficiency, making this an indispensable component in the preprocessing pipeline of brain imaging studies [5, 6].

The current gold standard in automatic brain extraction is a tool offered by the FMRIB Software Library (FSL), but manual intervention is often required to correct errors or adjust settings,

especially when dealing with scans exhibiting atypical features such as lesions or injuries or uncommon image sequences [7–9]. This FSL-BET tool faces several limitations, such as over-extraction leading to loss of brain matter, inaccurate extraction resulting in residual skull or non-brain tissue surrounding the brain to be falsely included in brain tissue, and sensitivity to image quality, which complicates its application on clinical images [10–12]. Furthermore, its restricted scope confines its utility to general brain extraction, without providing the capability to isolate specific regions or structures of the brain such as the corpus callosum, subcortical structures such as the basal ganglia that have different signal intensities, vascular structures within the brain, and other structures that might be of special interest.

As a result, numerous deep learning-based models have been developed for brain extraction and adjacent tasks. Despite this, there remains a significant demand for enhancing the accuracy of their results [13, 14]. As a consequence of their reliance on training data, these models have exhibited a lack of robustness [15].

The Segment Anything Model by Meta AI (SAM) has emerged as a state-of-the-art tool for image segmentation being trained over a vast dataset of 1 billion masks and 11 million images [16]. Its extensive training and zero-shot learning allowing it to respond appropriately to any prompt at inference time [17, 18]. SAM has already shown remarkable potential in accurately segmenting objects in real-world scenarios, such as road images featuring trees, vehicles, and pedestrians, and holding significant promise for enhancing autonomous vehicle systems. The model’s ability to analyze surveillance footage containing weapons, people, and cars offers potential improvements to security protocols. Additionally, in agriculture, particularly in segmenting plants and soil in aerial imagery or drone-captured photos, SAM enables precise crop growth analysis and identification of areas necessitating irrigation or fertilizing.

In this study, we conduct a comparative analysis of brain extraction techniques by evaluating SAM and the FSL-BET algorithm, which serves as a gold-standard in the field. We test both methods on a range of brain scans with varying image qualities, as well as different brain challenges caused by lesions and injuries. Additionally, we highlight the potential benefits that SAM may offer to neuroimaging researchers in comparison to existing techniques.

2 Methodology

2.1 Selection of MRI data

We examined 45 anonymized MR brain images comprising 9 different types obtained from various databases (ATLAS Data, white matter hyperintensities (WMH) Challenge Segmentation and our in-house dataset) [19, 20]. We encompassed a wide range of factors, including the various types of MRI sequences utilized, the quality of the images, the presence of any brain abnormalities, and the use of both normalized and non-normalized data.

2.2 Preprocessing of MRI data

To enable more accurate and reliable comparisons between the results obtained from BET and SAM, we resampled all the MRI data into MNI152 space[21]. This approach was intended to ensure all the data are aligned to a standardized reference template which is essential when performing group-level analyses and comparing results across different outputs.

2.3 Brain Extraction using FSL BET

FSL BET, a command-line tool, offers the convenience of using various parameters to enhance brain extraction in difficult or unusual cases, resulting in a customizable and semi-automated brain extraction process. The primary parameter which is used is the fractional intensity threshold (f) that determines the intensity level to distinguish between brain and non-brain tissue. By adjusting this value, we optimized the brain boundary estimation for the various data sets used in this paper. In some instances, we found that none of the f values effectively isolated the brain without either including a significant amount of non-brain tissue or excessively truncating the brain. In such cases, we reported the extraction results obtained using the default value. FSL BET is able to directly perform the brain extraction on 3D data, without requiring its conversion into 2D slices.

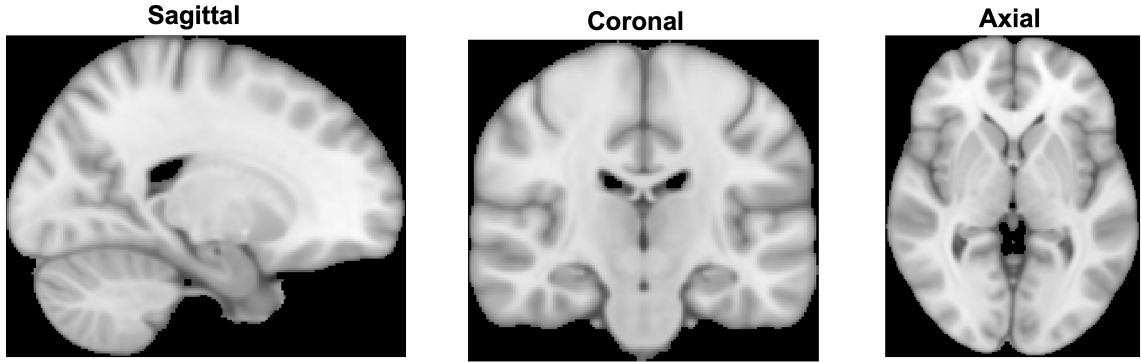


Fig. 1 Sagittal, coronal, and axial planes of MNI152 brain of size 1mm.

2.4 Brain Extraction using SAM

SAM, a deep learning model, facilitated the customization of the brain extraction process by enabling us to utilize various parameters, such as intensity threshold and spatial location, to selectively retain or remove different regions of the image. As a result, we were able to achieve a fully automated and highly customizable extraction process, not only for the brain but also for specific regions within the brain, such as the corpus callosum, subcortical structures (e.g., basal ganglia), vascular structures, and any other distinct brain structures of interest. In our case, we initially transformed each MRI scan into a set of 2D slices. Subsequently, we implemented a custom bounding box algorithm to accurately position markers, allowing us to effectively include a particular region or structure within the brain for extraction while simultaneously excluding regions not of interest based on voxel intensities. These inclusion and exclusion markers, alongside the 2D image slices, served as the set of inputs enabling precise mask generation from SAM.

2.4.1 3D MRI scan preprocessing and reconstruction

SAM requires 2D images as input, which we obtained by converting the processed MRI data into various 2D slices using the med2image Python tool. The predicted slices were then converted into the required brain extracted data using the nibabel Python library. Here is the schematic of the method we used to generate our final results:

1. Import Python Libraries
 - med2image
 - nibabel
2. Convert 3D MRI Data to 2D Slices
 - Specify desired slice orientation (axial, coronal, sagittal)
 - Use med2image to generate 2D slices
 - Save 2D slices as image files (e.g., PNG, JPEG)
3. Perform Prediction on 2D Slices (Using SAM)
 - Load trained model
 - Use Bounding Box Algorithm to generate input co-ordinates and inclusion or exclusion labels
 - Feed generated slices and markers to SAM to predict segmentations or desired features
 - Save the mask output for each slice
4. Reconstruct 3D Volume from 2D Slices
 - Stack the mask 2D slices to a 3D array
 - Reconstruct 3D volume with reference to the input brain affine transformation using nibabel
 - Save reconstructed brain-extracted data as a NIFTI file

2.5 Evaluation metrics for FSL BET and SAM output

We have evaluated our results over five different metrics to understand how the outputs from FSL BET and SAM have performed against the standard MNI152 1mm Brain images (as shown in Figure 1) which are used as the ground truth of a dataset that only contains brain tissue.

1. **Dice coefficient:** A similarity metric that evaluates the overlap between two binary images, namely the extracted brain and the ground truth. Higher values of the Dice coefficient indicate better performance of the brain extraction technique.
2. **Jaccard Index:** Also known as the Intersection over Union (IoU), this is another similarity metric that measures the overlap between two binary images. Similar to the Dice coefficient, higher values of the Jaccard Index indicate better performance of the brain extraction technique.
3. **Accuracy:** An evaluation metric that calculates the proportion of correctly classified instances out of the total number of instances.
4. **Precision:** A metric that measures the proportion of true positives out of all extracted positives, in comparison to the ground truth. It enables an assessment of the accuracy of the brain extraction technique in identifying actual brain tissue.
5. **Recall:** This calculates the proportion of true positives out of all actual positives when compared against the ground truth, enabling the assessment of the ability of the brain extraction technique to detect all actual brain tissue.

3 Results

3.1 Evaluation of Extractions by FSL BET and SAM

The brain extractions performed by FSL BET and SAM were evaluated across the five aforementioned metrics, compared against ground truth. Our analysis showed that, in the majority of cases, the brain extractions produced using SAM were superior to those generated by BET, as evidenced by our evaluation metrics and accompanying figures from different imaging modalities. Detailed results from additional brain extraction techniques, along with their corresponding evaluation metrics, have been included in the supplementary document.

Table 1 Comparison of accuracy, precision, and recall values for 9 different types of brain images. The source of the data is mentioned in parentheses below the type of image. The numbers in bold indicate the value of the metric, and the model, which is better, for the specific brain image type.

Types of Brain Images	BET			SAM		
	Accuracy	Precision	Recall	Accuracy	Precision	Recall
T1-weighted images from Acute Stroke Phase (ATLAS [19])	0.919	0.901	0.963	0.951	0.961	0.972
T2-weighted images from Chronic Stroke Phase (in-house)	0.958	0.981	0.963	0.962	0.982	0.968
FLAIR images from Chronic Stroke Phase (in-house)	0.883	0.899	0.927	0.937	0.981	0.93
Normalized T2-weighted images from Chronic Stroke Phase (in-house)	0.761	0.999	0.761	0.967	0.998	0.961
Normalized FLAIR images from Chronic Stroke Phase (in-house)	0.757	0.757	0.999	0.887	0.884	0.964
FLAIR images from WMH Challenge Set [20]*	0.879	0.784	0.824	0.737	0.777	0.833
3DT1-weighted images from WMH Challenge Set [20]	0.396	0.127	0.982	0.852	0.961	0.846
T1-weighted images from WMH Challenge Set [20]	0.839	0.881	0.906	0.916	0.972	0.921
Fractional Anisotropy (FA) images from Chronic Stroke Phase (in-house)	0.484	0.321	0.998	0.88	0.874	0.965

*Case of under cropping for which the evaluation metrics are misleading.

Table 2 Comparison of Dice Coefficient and Jaccard Index distance value for 9 different types of brain images. The source of the data is mentioned in parentheses below the type of image. The numbers in bold indicate the value of the metric, and the model, which is better, for the specific brain image type.

Types of Brain Images	BET		SAM	
	Dice Coefficient	IoU	Dice Coefficient	IoU
T1-weighted images from Acute Stroke Phase (ATLAS [19])	0.929	0.869	0.966	0.935
T2-weighted images from Chronic Stroke Phase (in-house)	0.972	0.946	0.975	0.951
FLAIR images from Chronic Stroke Phase (in-house)	0.913	0.849	0.955	0.914
Normalized T2-weighted images from Chronic Stroke Phase (in-house)	0.865	0.761	0.979	0.959
Normalized FLAIR images from Chronic Stroke Phase (in-house)	0.862	0.758	0.922	0.856
FLAIR images from WMH Challenge Set [20]*	0.923	0.839	0.803	0.672
3DT1-weighted images from WMH Challenge Set [20]	0.226	0.127	0.899	0.817
T1-weighted images from WMH Challenge Set [20]	0.893	0.807	0.946	0.898
Fractional Anisotropy (FA) images from Chronic Stroke Phase (in-house)	0.485	0.321	0.917	0.847

*Case of under cropping for which the evaluation metrics are misleading.

3.2 Accuracy, Precision and Recall

The results in Table 1 indicate that BET performs well on high-quality images that are devoid of lesions and have been spatially normalized to a standard space. However, when dealing with images of good quality but with lesions located near the outer contour of the brain or in regions that are difficult to differentiate from surrounding meninges, the performance of BET suffers. In contrast, the custom bounding box algorithm implemented in SAM allowed for the inclusion and exclusion of specific markers, resulting in consistently superior performance across all image qualities and brain abnormalities. For example, in the WMH 3DT1 dataset, SAM achieved an accuracy of 0.852, a precision of 0.961, and a recall of 0.846, compared to BET’s accuracy of 0.396, precision of 0.127, and recall of 0.982. These results demonstrate a superior performance of SAM over BET.

3.3 Dice Coefficient and Jaccard index

Table 2 confirms our earlier findings presented in Table 1, which indicate that BET demonstrated strong performance when applied to high-quality images without lesions located near the outer boundaries of the brain or in proximity to the meninges. However, SAM consistently outperformed BET in brain extraction across all variations. In one particular case from the WMH 3DT1 dataset, BET significantly underperforms (due to gross over-cropping), achieving a dice-coefficient of 0.226 and a Jaccard index of 0.127, compared to SAM’s output that achieves a dice-coefficient of 0.899 and a Jaccard index of 0.817.

3.4 Visual Comparison

Our findings from the figures are consistent with those presented in Tables 1 and 2, whereby BET exhibited superior performance in cases involving high-quality images and normalized data, whereas SAM consistently outperformed BET across all variations. For instance, Figure 2 depicts the T1 scan from an acute stroke patient in the ATLAS v2.0 dataset, along with its corresponding BET output and SAM output across three different planes: sagittal, coronal, and axial. Similarly, in other figures, we observe one of the planes of the brain, along with the corresponding BET and SAM output.

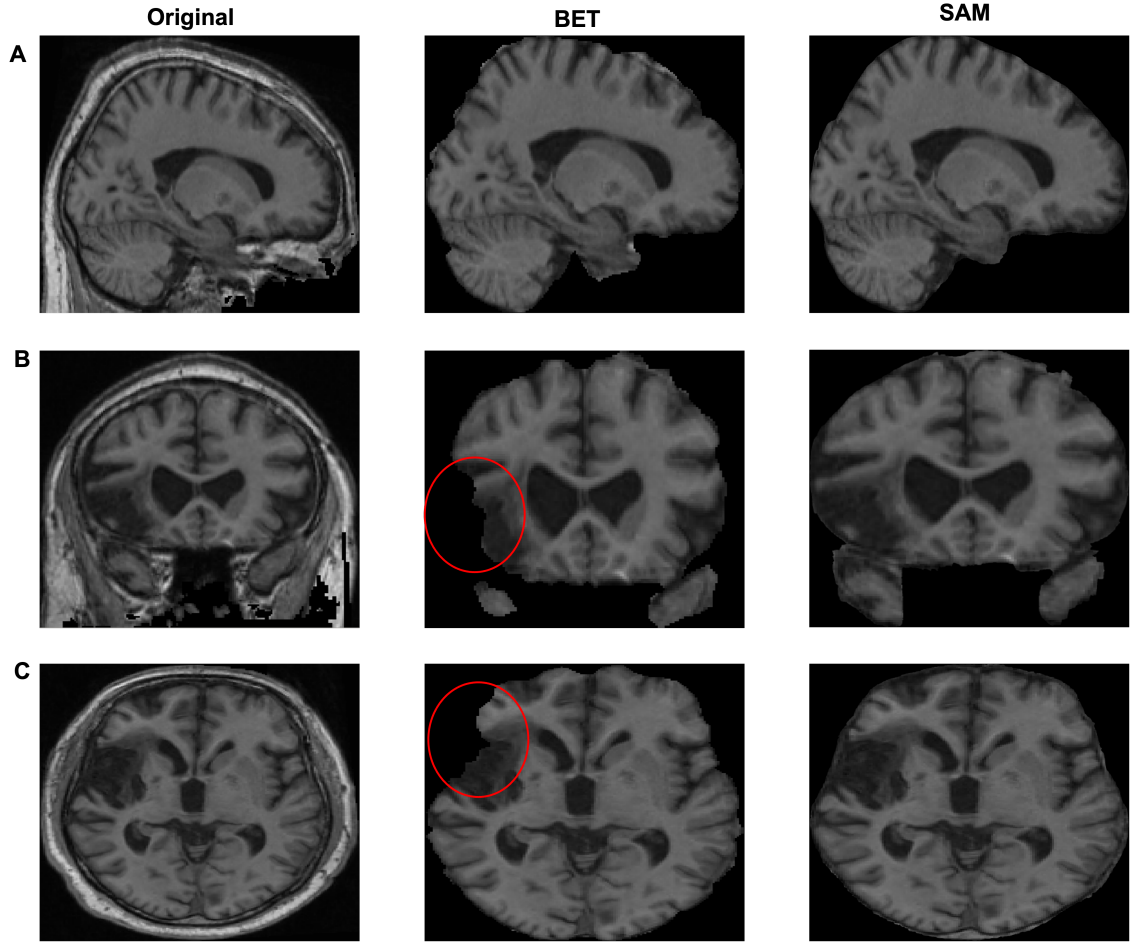


Fig. 2 Comparison of original MRI images and extraction outputs by BET and SAM for **A.** sagittal, **B.** coronal, and **C.** axial anatomical planes. BET extraction results in sagittal, coronal, and axial planes, respectively. SAM extraction results in sagittal, coronal, and axial planes, respectively. The data is from ATLAS v2.0 dataset [19].

As illustrated in Figure 3, when dealing with high-quality images, both BET and SAM produced comparable brain extractions for high resolution normalized T2-weighted images (3A), but BET struggled with clearly separating non-brain tissue from the brain in normalized sagittal FLAIR images (3B). BET performed poorly in non-normalized T1-weighted images with small vessel lesions in which only portions of the brain tissue was extracted while SAM did a superior job (3C). Finally, it is worth noting that inhomogeneous and poor contrast Fractional Anisotropy images derived from a large set of raw diffusion tensor images in which diffusion gradients at a b-value of 1000 were applied in 30 directions while acquiring a corresponding set of b-0 images, were competently extracted by SAM preserving all brain tissue, while FSL BET cropped major portions of the brain.

4 Discussion

The results of our study provided valuable comparative insights into the effectiveness and various potential applications and challenges of a new method of brain extraction, SAM, with FSL BET, a gold-standard in the field of brain extraction. The primary objective of our study was to examine the performance of these tools in the context of brain extraction and provide an overview of how effective SAM is in segmenting the specific regions of interest. Our findings support the utility of these tools for specific tasks of image pre-processing as well as detailed within-image processing and analysis.

In accordance with our research question, the study has shown that both the SAM and FSL BET are capable of accurately extracting brain structures from a variety of brain types to a certain degree of error. In addition, the comparison of these tools has revealed that SAM has outperformed

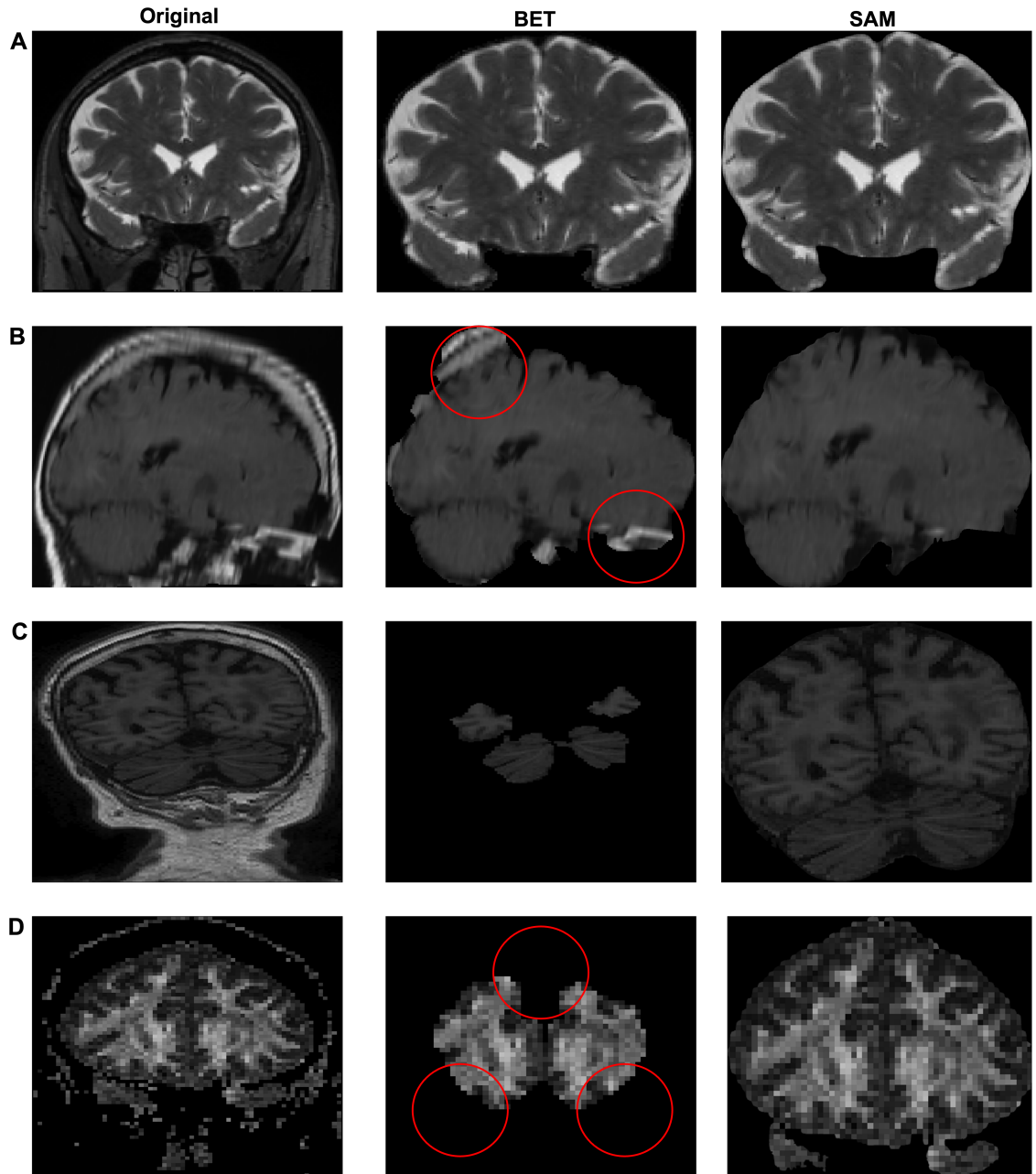


Fig. 3 Comparison of original MRI images and extraction outputs by BET and SAM for **A.** T2 scan from a chronic stroke patient in the coronal plane, **B.** FLAIR scan from a chronic stroke patient in the sagittal plane, **C.** 3DT1 scan from a patient having WMH in the coronal plane, and **D.** FA scan from a patient having chronic stroke in the coronal plane. Data for **A.**, **B.** and **D.** are from in-house dataset, and **C.** is from WMH challenge dataset [20].

FSL BET in terms of various evaluation parameters for many of the tested cases. This suggests that SAM could potentially be a more suitable tool for brain extraction, segmentation, and identification of specific regions in neuroimaging research.

4.1 Advantages and Limitations of SAM and FSL BET

One of the key advantages of SAM is its flexibility and adaptability to different types of data. Since the model has been trained on a huge number of images, it enables it to adapt to various imaging modalities and contrasts, making it a versatile tool for a wide range of neuroimaging applications. Moreover, SAM's impressive performance on various evaluation parameters attests to its reliability and efficacy in brain extraction, and its ability to identify specific brain regions, such as the corpus

callosum, subcortical structures, vascular structures, and other specialized areas makes it a highly versatile tool.

Nonetheless, it is important to note that the conversion of 3D MRI data to 2D slices and subsequent reconstruction, which is required for using SAM, represents a potential drawback in MRI analysis. Moreover, processing the data using SAM entails high computational resources, such as GPUs and large RAM, and the entire pipeline, from converting 3D data to running SAM on 2D slices and performing reconstruction, can take approximately 30 seconds.

FSL BET's strength lies in the simplicity and robustness, rendering it a reliable tool for brain extraction particularly when brains are in a spatially normalized space. However, our study validated that its accuracy and precision may be inferior to that of SAM in certain scenarios, such as when the image quality is suboptimal, has poor contrast, unnormalized, or when images contain brain lesions that are located near the outer portions of the brain. Moreover, unlike SAM, FSL BET is unable to efficiently segment and extract specific brain sub-regions, which limits its application to primarily full brain extraction.

4.2 Potential Applications of SAM segmenting particular brain structures and lesions

Given its versatility, the potential applications of SAM in neuroimaging research are vast. This tool could be used for automating the various preprocessing pipelines required in imaging data for large scale studies like those investigating neurodegenerative diseases or brain development. Additionally, its ability to accurately segment and extract brain structures, as well as identifying specific regions of interest, could accelerate a lot of the studies involving structure-function relationships. This could also lead to contributing to the development of personalized medicines in neurology and psychiatry. As demonstrated in Figure 4, we show examples of how SAM could also be utilized for precise segmentation of lesions, bleeds within brain tissue, midsagittal corpus callosum size, and size/volumes of ventricles.

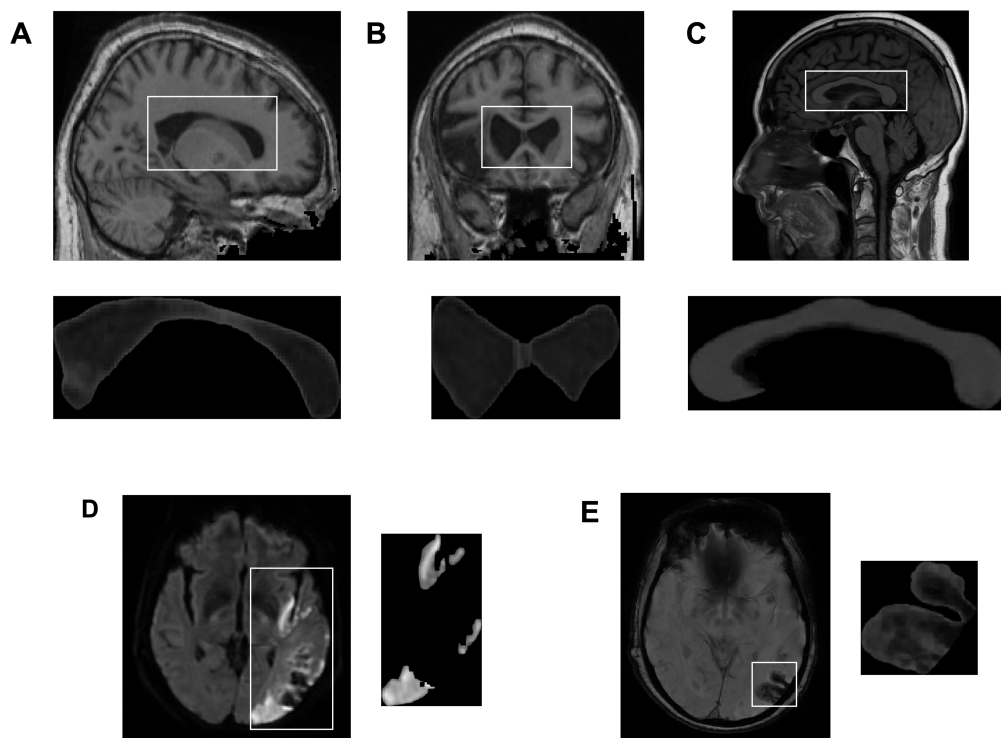


Fig. 4 A., B. Ventricles extracted from a T1 scan from acute stroke phase. C. Corpus callosum extracted from a 3DT1 scan from chronic stroke phase. D. Lesions extracted from a DWI scan from chronic stroke phase. E. Microbleeds extracted from a SWAN scan from chronic stroke phase. Data in A. and B. are from ATLAS v2.0 [19], and C., D., and E. are from in-house dataset.

4.3 Future Work

Future research in this area should concentrate on addressing the existing limitations of SAM, such as exploring various reconstruction techniques to optimize its performance for 3D image datasets, as well as further exploring its potential applications in neuroimaging research. To enhance the robustness and generalizability of SAM across a broad range of contextual tasks, including fast and precise lesion segmentation, segmentation of clinically relevant structures within the brain, as well as lesion progression and therapy responses. Considering all of these possibilities, fine-tuning the model will require a diverse and comprehensive training dataset that covers various neuroimaging modalities and pathologies.

5 Conclusion

Our findings provide evidence of the significant additional potential of SAM in comparison with FSL BET in pre-processing as well as detailed within-brain image analysis, in particularly brain extraction from the skull and meninges even in challenging cases with lesions involving the outer parts of the brain, brain tissue segmentation allowing the differentiation of lesioned from non-lesioned tissue components, and rapid identification and delineation of specific regions of interest. Our evaluation metrics indicate that SAM consistently outperforms FSL BET, demonstrating its superior performance across a broad range of imaging modalities and pathologies. Our ongoing research will identify any limitations that SAM might pose and will aim to further improve its effectiveness and generalizability across a wide array of neuroimages. Advancements in the image preprocessing as well as image segmentation field can lead to a deeper understanding of brain structure and function and can facilitate the development of more precise and effective diagnostic approaches and has the potential to advance therapeutic options. Overall, our study underscores the value of cutting-edge deep learning techniques to advance the field of applied and translational neuroimaging.

Supplementary Information

Here is the link to the supplementary document referenced in this paper: shorturl.at/bACZ9

Acknowledgement

This research was supported by NIMH (Brain-Initiative) (7R01MH111874-05). GS also acknowledges support from NINDS (U01NS102353). SM acknowledges the support from IALS summer internship program (direct summer stipend support). Conflict of interest statement: GS is the co-founder of Brainify, LLC, and has ownership interest in Brainify, LLC. Brainify LLC financially supported the research conducted in this study, but had no influence on data processing or the derived results or the presentation or interpretation of the results.

References

- [1] Despotovic, I., Goossens, B. & Philips, W. Mri segmentation of the human brain. *Challenges, Methods, and Applications, Computational and Mathematical Methods in Medicine* **2015** (2015).
- [2] Ashburner, J. *et al.* Computer-assisted imaging to assess brain structure in healthy and diseased brains. *The Lancet Neurology* **2**, 79–88 (2003).
- [3] Somasundaram, K. & Kalaiselvi, T. Fully automatic brain extraction algorithm for axial t2-weighted magnetic resonance images. *Computers in biology and medicine* **40**, 811–822 (2010).
- [4] Thompson, P. M. *et al.* Detection and mapping of abnormal brain structure with a probabilistic atlas of cortical surfaces. *Journal of computer assisted tomography* **21**, 567–581 (1997).
- [5] Van der Kouwe, A. J., Benner, T., Salat, D. H. & Fischl, B. Brain morphometry with multiecho mprage. *Neuroimage* **40**, 559–569 (2008).
- [6] Fein, G. *et al.* Statistical parametric mapping of brain morphology: sensitivity is dramatically increased by using brain-extracted images as inputs. *Neuroimage* **30**, 1187–1195 (2006).
- [7] Smith, S. M. Fast robust automated brain extraction. *Human brain mapping* **17**, 143–155 (2002).
- [8] Jenkinson, M., Beckmann, C. F., Behrens, T. E., Woolrich, M. W. & Smith, S. M. Fsl. *Neuroimage* **62**, 782–790 (2012).
- [9] Battaglini, M., Smith, S. M., Brogi, S. & De Stefano, N. Enhanced brain extraction improves the accuracy of brain atrophy estimation. *Neuroimage* **40**, 583–589 (2008).
- [10] Zhuang, A. H., Valentino, D. J. & Toga, A. W. Skull-stripping magnetic resonance brain images using a model-based level set. *NeuroImage* **32**, 79–92 (2006).
- [11] Klein, A. *et al.* Evaluation of volume-based and surface-based brain image registration methods. *Neuroimage* **51**, 214–220 (2010).
- [12] Boesen, K. *et al.* Quantitative comparison of four brain extraction algorithms. *NeuroImage* **22**, 1255–1261 (2004).
- [13] Pei, L. *et al.* A general skull stripping of multiparametric brain mris using 3d convolutional neural network. *Scientific Reports* **12**, 10826 (2022).
- [14] Fatima, A., Shahid, A. R., Raza, B., Madni, T. M. & Janjua, U. I. State-of-the-art traditional to the machine-and deep-learning-based skull stripping techniques, models, and algorithms. *Journal of Digital Imaging* **33**, 1443–1464 (2020).
- [15] Thakur, S. *et al.* Brain extraction on mri scans in presence of diffuse glioma: Multi-institutional performance evaluation of deep learning methods and robust modality-agnostic training. *NeuroImage* **220**, 117081 (2020).
- [16] Kirillov, A. *et al.* Segment anything. *arXiv preprint arXiv:2304.02643* (2023).
- [17] He, K. *et al.* Masked autoencoders are scalable vision learners. *Proceedings of the IEEE/CVF Conference on Computer Vision and Pattern Recognition* 16000–16009 (2022).
- [18] Xian, Y., Lampert, C. H., Schiele, B. & Akata, Z. Zero-shot learning—a comprehensive evaluation of the good, the bad and the ugly. *IEEE transactions on pattern analysis and machine intelligence* **41**, 2251–2265 (2018).

- [19] Liew, S.-L. *et al.* A large, open source dataset of stroke anatomical brain images and manual lesion segmentations. *Scientific data* **5**, 1–11 (2018).
- [20] Kuijf, H. J. *et al.* Standardized assessment of automatic segmentation of white matter hyperintensities and results of the wmh segmentation challenge. *IEEE transactions on medical imaging* **38**, 2556–2568 (2019).
- [21] Evans, A. C., Janke, A. L., Collins, D. L. & Baillet, S. Brain templates and atlases. *Neuroimage* **62**, 911–922 (2012).